EVOLUTION OF THE $4f$ ELECTRON LOCALIZATION FROM YbRh$_2$Si$_2$ to YbRh$_2$Pb STUDIED BY ELECTRON SPIN RESONANCE

V. A. Ivanshin [a,c]*, **T. O. Litvinova** [a], **N. A. Ivanshin** [b],

A. Pöppl [c], **D. A. Sokolov** [d], **M. C. Aronson** [e,f]

[a] *MRS Laboratory, Kazan Federal (Volga Region) University*
420008, Kazan, Russia

[b] *Kazan State University of Architecture and Engineering*
420043, Kazan, Russia

[c] *Faculty of Physics and Earth Sciences, University of Leipzig*
D-04103, Leipzig, Germany

[d] *School on Physics and CSEC, University of Edinburgh*
EH 3JZ, Edinburgh, UK

[e] *Department of Physics and Astronomy, Stony Brook University*
11794-3800, Stony Brook, NY, USA

[f] *Condensed Matter Physics and Materials Department, Brookhaven National Laboratory*
11973-5000, Upton, NY, USA

We report electron spin resonance (ESR) experiments on the Heusler alloy YbRh$_2$Pb and compare its spin dynamics with that of several other Yb-based intermetallics. A detailed analysis of the derived ESR parameters indicates the extremely weak hybridization, more localized distribution of the $4f$ states, and a smaller RKKY interaction in YbRh$_2$Pb. These findings reveal the important interplay between hybridization effects, chemical substitution, and crystalline electric field interactions that determines the ground state properties of strongly correlated electron systems.

1. INTRODUCTION

One interesting aspect of the heavy-fermion (HF) compounds is the evolution from high-temperature unscreened localized f electrons to itinerant heavy quasiparticles with effective masses hunderds of times that of bare electrons at low temperature [1]. Recent experimental and theoretical studies on the HF Yb-based materials have revealed a rich physics of transport and magnetic properties of these systems (see, e. g., Ref. [2] for a review). In principle, the Yb systems are the $4f$-hole analogue of the Ce-based compounds [3] and their ground state properties strongly depend on the Yb valence and the strength of hybridization between the $4f$ electrons (holes) and the conduction d-, p-, or s-electrons. The most essential role belongs here, on the one hand, to the Kondo coupling that screens the Yb or Ce magnetic moment and creates a paramagnetic ground state with enhanced masses of quasiparticles and, on the other hand, to the Ruderman–Kittel–Kasuya–Yoshida (RKKY) exchange interaction, which causes a magnetic ordering [4]. A key for understanding the behavior of HF compounds is the interplay between both these phenomena. At a low value of Kondo exchange, the conduction electrons are carriers of long-range magnetic interactions, and the local moments of f shells are ordered in the weak Kondo coupling limit. With an increase in the Kondo effect, the ordered state is suppressed, creating a screening of moments in the strong Kondo coupling regime. As presented on the Doniach phase diagram [5], a quantum phase transition occurs between these two regimes.

*E-mail: Vladimir.Ivanshin@kpfu.ru

The ESR technique could directly probe the local moments of f electrons and their interaction with conduction electrons [6]. However, as a rule, no concentrated HF systems (including Kondo lattices) can be studied using ESR because of a very fast relaxation of the resonating spin, which leads to a huge ESR linewidth, too broad to be observable and proportional to the Kondo temperature. One expects the ESR to be washed out by the Kondo effect because the lattice of local moments is strongly coupled to conduction electrons. Therefore, it is necessary to dope small amounts of ions with localized magnetic moments, such as Ce^{3+} or Gd^{3+}, into the compound under investigation. Surprisingly, during the last two decades, the low-temperature ESR signals have been detected in some undoped Yb-based intermetallics, e. g., mixed-valence compound YbCuAl [7], quantum critical system $YbRh_2Si_2$ [8], its parent compounds $YbIr_2Si_2$ [9] and $YbCo_2Si_2$ [10], and in several other Ce- and Eu-based alloys [11].

Different theoretical approaches [12–15] show that the narrow anisotropic ESR can be observed in some dense HF compounds in a broad range of magnetic fields as a result of hybridization between $4f$ and conduction electrons in conjunction with ferromagnetic (FM) fluctuations [16], which can significantly reduce the ESR linewidth and make it observable. Finally, very recent results of inelastic neutron scattering experiments [17] explain the ESR mode in $YbRh_2Si_2$ as a mesoscopic spin resonance of localized droplets of Yb^{3+} spins and conduction electrons due to a coherent precession of the spin density, extending the distance 6 ± 2 Å beyond the Yb site. Such ESR absorption is not caused by the purely localized Yb^{3+} ions and is not associated with correlated effects over long length scales. In this work, the spin dynamics in $YbRh_2Pb$ probed by ESR is compared to that of some relative Yb materials.

2. EXPERIMENTAL PROCEDURE

Samples of $YbRh_2Pb$ were obtained from Pb flux as described previously in [18]. They crystallize in a distorted Heusler alloy structure with dimensions $a = 4.5235(4)$ Å and $c = 6.9864(6)$ Å, and a probable space group $I4/mmm$. The ESR spectra (ESR linewidth $\Delta H = 600$–2300 Oe) were taken in the Bruker ESM/plus X-band (9.4 GHz) [19] and in the EMX 10–40 Q-band (34.1 GHz) spectrometers. In both cases, we used the Oxford continuous-flow liquid-helium cryostats in the temperature range
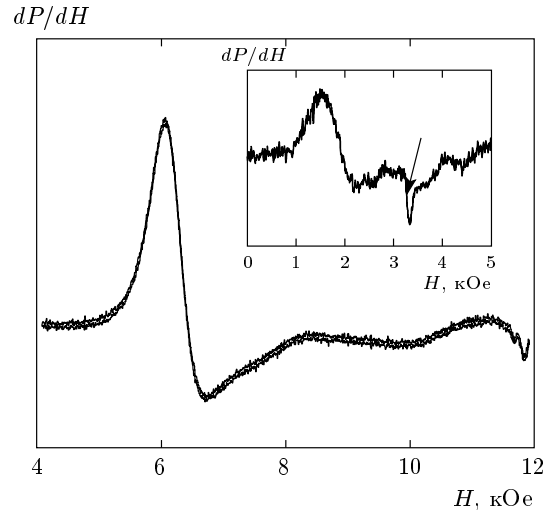

Fig. 1. Derivative of the absorption ESR signal at $T = 5$ K at the Q-band frequency (34.1 GHz) in $YbRh_2Pb$. Inset: The X-band (9.45 GHz) ESR spectrum at $T = 4.2$ K. The arrow indicates the parasitic signal from the microwave cavity

4.2 K $\leq T \leq 25$ K. Above 25 K, no ESR signal was observed. A multiply twinned crystal structure of the investigated small grains (1–2 mm^2 surface area), which was established with a Bruker Smart charged-coupled device X-ray diffractometer, has prevented an orientation of samples and an accurate determination of the local symmetry of paramagnetic centers.

The X- and Q-band ESR spectra of $YbRh_2Pb$ are shown in Fig. 1 for 5 K. The intensity of the X-band ESR spectrum was comparable with that of the cavity background signal, which is indicated by arrow on the inset in Fig. 1. Its intensity was approximately 20–30 times smaller than that for $YbRh_2Si_2$ as measured by identical experimental conditions on the samples of very similar size and weight [8, 20]. The measurements at the Q-band frequency allowed us to obtain a higher resolution of the ESR line with a much better signal-to-noise ratio.

No significant deviation from the linear behavior was observed below 15 K for the temperature dependence of the ESR linewidth ΔH at the Q-band frequency (Fig. 2). On a further increase in temperature, the ESR lineshape was essentially distorted, and this was accompanied by an even faster increase in its linewidth. The temperature dependences of the ESR g-factor are given in Fig. 3 for both frequencies.

7*
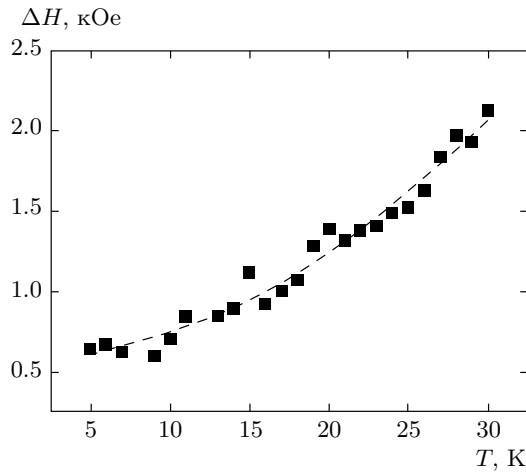
Fig. 2. Temperature evolution of the ESR linewidth at 34.1 GHz in $YbRh_2Pb$. The dashed line is the theoretical curve obtained from Eq. (1)
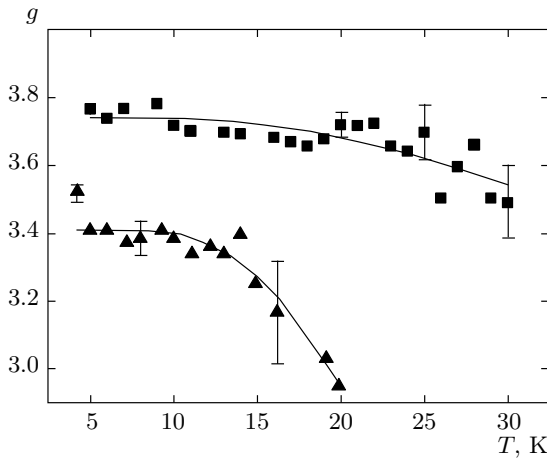
Fig. 3. Temperature effective ESR g-factor dependence for X-band at 9.45 GHz (triangles) [19] and Q-band at 34.1 GHz (squares) in $YbRh_2Pb$. Solid lines represent the best fits using Eq. (2)

3. DISCUSSION

We suppose that the ESR signal in $YbRh_2Pb$ originates from the hybridization of $4f$ Yb electrons with conduction electrons in the presence of FM fluctuations, as was also proposed for $YbRh_2Si_2$ and $YbIr_2Si_2$ [8,9]. In accordance to Refs. [8] and [20], the temperature dependence of ΔH of ESR spectra in $YbRh_2Pb$ at 34.1 GHz can be well fitted (see the dashed line in Fig. 2) by the formula

$$\Delta H = A + BT + C\exp(-\Delta/T),　　　(1)$$

where the measured Korringa rate $B \approx 27 \pm 2$ Oe/K is within the usual order of magnitude of ytterbium, and the activation energy of the first excited Stark sublevel of the Yb^{3+} ion is $\Delta \approx 73.5$ K. This value of Δ corresponds very well to the estimation of the first excited crystal electric field level of this ion, $\Delta_1 = 68 \pm 5$ K, which has been derived after heat capacity and magnetic susceptibility measurements in $YbRh_2Pb$ [18]. The residual ESR linewidth A changes approximately from 420 to 470 Oe upon passing from the X- to the Q-band experiments. Finally, the parameter $C = 69.5 \pm 2$ kOe (X-band) [19] or 9.0 ± 1 kOe (Q-band). The exponential term is caused by random transitions from the ground sublevel of the Yb^{3+} ion to the first excited crystal electric field level separated by the distance Δ [8]. This electronic mechanism of thermal fluctuations can nicely explain the temperature dependence of the effective ESR g-factor in $YbRh_2Pb$ above 10 K (see Fig. 3), also with the same value $\Delta \approx 73.5$ K, using the expression

$$g(T) = g_0 + \Delta g_0 \exp(-\Delta/T),　　　(2)$$

where $\Delta g_0 = g_{exc} - g_0$, g_0 and g_{exc} are respectively the effective ESR g-factors of the ground and first excited sublevels of the ytterbium ion. At the Q-band frequency, $\Delta g_0 = -2.23$ and $g_{exc} = 1.509$ are found to be more reasonable values than those reported after the fitting procedure of the X-band ESR spectra in $YbRh_2Pb$ ($\Delta g_0 = -18.5$ and $g_{exc} = -15.1$) [19]. A huge difference between both sets of the parameters is caused by errors during simulation of the extremely broad and weak X-band ESR signals in the temperature range between 13 and 20 K. Moreover, both these Q-band values are in close agreement with the corresponding fitting parameters obtained from the Q-band ESR experiments on $YbRh_2Si_2$ [8], $\Delta g_0 = -2.58$ and $g_{\perp}^{exc} = 1.0$. Recently, Ramires and Coleman [15] showed that a very similar ESR g-factor shift with temperature in the another HF metal β-$YbAlB_4$ can be understood as a result of the development of a coherent many-body hybridization between conduction electrons and the localized f states. This approach is related to the intermediate value of the crystal electric field excitations, which are comparable to the hybridization strength.

Therefore, the ESR of $YbRh_2Pb$ can be associated with the field-split ground-state doublet of the Yb^{3+} ions, as was also predicted in $YbRh_2Si_2$ [8,17], $YbIr_2Si_2$ [9], and $YbRh_6P_4$ [21]. The localized droplets of the Yb^{3+} spins, which were induced by a magnetic field, are resonantly excited through crystal electric field intradoublet transitions. The spin dynamics in $YbRh_2Pb$

at $T > 10$ K can be attributed to the spin–lattice relaxation via the hybridized first excited crystal electric field state of the Yb^{3+} ion at $\Delta \approx 73.5$ K. This conclusion contradicts the findings of the high-frequency ESR studies at 360 GHz in $YbRh_2Si_2$ [22], where the strong broadening of the ESR response above 15 K in $YbRh_2Si_2$ was explained by the breakdown of the HF state only because of a huge difference between the positions of the Yb^{3+} — the first excited state measured in $YbRh_2Si_2$ by ESR technique and inelastic neutron scattering (INS). However, an effective hybridization of the $4f$ electrons with conduction electrons in the strongly hybridized HF materials $YbRh_2Si_2$ and $YbIr_2Si_2$ significantly broadens the otherwise atomically sharp f states (in contrast to the usual intermetallics $YbRh_2Pb$ and $YbRh_6P_4$ with a much weaker hybridization, for example). Therefore, the positions of all excited states of Yb^{3+} in $YbRh_2Si_2$ and $YbIr_2Si_2$ have been estimated from the INS studies as an extremely small humps on a very broad (80–100 K) shoulders [23, 24]. The lowest part of such a shoulder only can be involved in the electronic spin–lattice relaxation and can be measured from the ESR experiments directly with a significant deviation from the central position of the shoulder [8, 19]. By contrast, a very weak extent of hybridization effects in $YbRh_2Pb$ leads to a more accurate determination of the first excited crystal electric field level of Yb^{3+} during ESR studies.

The hybridization strength strongly depends on chemical composition. A comparison of the ESR data in $YbRh_2Pb$, $YbRh_2Si_2$, and $YbIr_2Si_2$ allows estimating possible effects of the f–d–p hybridization on the spin dynamics. Apart from the chemically inactive core electrons, Si ($[Ne]3s^23p^2$) and Pb ($[Hg]6p^2$) are isoelectronic. Indeed, the ESR measurements show very similar spin–lattice relaxation processes in $YbRh_2Pb$ and $YbRh_2Si_2$. However, the extremely weak f–p hybridization in $YbRh_2Pb$ causes a very low intensity of ESR signals, probably, as a result of a much lower efficiency of the mixing between the $4f$- and $6p$-shells in comparison with the strong $4f$–$3p$ hybridization in $YbRh_2Si_2$. Further, the substitution of Rh ($[Kr]4d^85s^2$) by Ir ($[Xe]5d^76s^2$), having one d electron less than Rh, in $YbIr_2Si_2$ leads to a reduced contribution of conduction electrons to the ESR relaxation mechanism in comparison with $YbRh_2Si_2$ [9, 20]. A vanishingly small RKKY interaction among magnetic moments and a weakened f–d–p hybridization with the absence of correlation effects among the conduction electrons [18] suggest that relatively small FM droplets of the Yb^{3+} moments are more localized in $YbRh_2Pb$ than in the quantum critical systems $YbRh_2Si_2$, $YbIr_2Si_2$, and β-$YbAlB_4$, in which the most intense ESR signals have been observed. A possible close relation of quantum criticality to observation of a sharp well-defined f-electron ESR lines is one of the unresolved problems in the physics of HF metals [15]. A delicate balance between the Kondo coupling of the localized $4f$ electrons to the conduction electrons and spin–orbit coupling compared with the crystal electric field interaction can be tuned by doping or by pressure and can lead to the appearance of a quantum phase transition [25, 26]. Thus, the substitution of silicon with lead atoms by passing from $YbRh_2Si_2$ to $YbRh_2Pb$ changes the f–p hybridization and a possible distance to the quantum critical point. We believe that $YbRh_2Pb$ belongs to the weak-coupling limit of the Doniach phase diagram [5], and the small but finite temperature magnetic phase transition observed in $YbRh_2Pb$ [18] limits any non-Fermi liquid behavior to very small reduced temperatures.

Several communications devoted to the detection of ESR in a variety of dense intermetallics with a possible strong f–d–s–p hybridization effects have been published during the last five years. The ESR absorption has been found not only in the typical HF materials such as $YbBiPt$, YbT_2Zn_{20} (T = Co, Fe) [27], β-$YbAlB_4$ [6] or in the borides CeB_6 [13, 28–30] and EuB_6 [31] with strong low-energy FM fluctuations, but also in the Kondo lattice $CeRuPO$ and in the alloy $YbRh$ that exhibit a static FM order [16]. These observations appear to be supported by FM correlations, and a sharp ESR signals may exist in many other intermetallic systems. The probable connection between intense ESR spectra and quantum critical effects should be a subject for further investigations. Therefore, the ESR technique can be a very powerful tool in studying hybridization effects in different itinerant ferromagnets in addition to methods such as INS, X-ray-, and photoemission spectroscopy.

REFERENCES

1. A. C. Hewson, *The Kondo Problem to Heavy Fermions*, Cambridge Univ. Press, Cambridge (1993).

2. M. C. Aronson, M. S. Kim, M. C. Bennett et al., J. Low Temp. Phys. **161**, 98 (2010).

3. R. Boursier, A. Villaume, G. Lapertot et al., Physica B **403**, 726 (2008).

4. G. R. Stewart, Rev. Mod. Phys. **56**, 755 (1984).

5. S. Doniach, Physica B + C **91**, 231 (1977).

6. L. M. Holanda, J. M. Vargas, W. Iwamoto et al., Phys. Rev. Lett. **107**, 026402 (2011).

7. C. Tien, J.-T. Yu, and H.-M. Du, Jpn. J. Appl. Phys. **32**, 2658 (1993).

8. V. A. Ivanshin, L. K. Aminov, I. N. Kurkin et al., Pis'ma v Zh. Eksp. Teor. Fiz. **77**, 625 (2003).

9. J. Sichelschmidt, J. Wykhoff, H.-A. Krug von Nidda et al., J. Phys.: Condens. Matter **19**, 016211 (2007).

10. T. Gruner, J. Sichelschmidt, C. Klingner et al., Phys. Rev. B **85**, 035119 (2012).

11. V. A. Ivanshin, T. O. Litvinova, and A. A. Sukhanov, J. Phys.: Conf. Ser. **273**, 012035 (2011).

12. E. Abrahams and P. Wölfle, Ann. Phys. (Berlin) **523**, 591 (2011).

13. P. Schlottmann, J. Appl. Phys. **113**, 175E109 (2013).

14. D. Huber, Mod. Phys. Lett. B **29**, 1230021 (2012).

15. A. Ramires and P. Coleman, arXiv:cond-mat/1307.4109v1.

16. C. Krellner, T. Förster, H. Jeevan et al., Phys. Rev. Lett. **100**, 066401 (2008).

17. C. Stock, C. Broholm, F. Demmel et al., Phys. Rev. Lett. **109**, 127201 (2012).

18. D. A. Sokolov, M. S. Kim, M. C. Aronson et al., Phys. Rev. B **77**, 174401 (2008).

19. V. A. Ivanshin, T. O. Litvinova, A. A. Sukhanov et al., Pis'ma v Zh. Eksp. Teor. Fiz. **90**, 126 (2009).

20. J. Sichelschmidt, V. A. Ivanshin, J. Ferstl et al., Phys. Rev. Lett. **91**, 156401 (2003).

21. V. A. Ivanshin, E. M. Gataullin, A. A. Sukhanov et al., J. Phys.: Conf. Ser. **291**, 012024 (2012).

22. U. Schaufuß, V. Kataev, A. A. Zvyagin et al., Phys. Rev. Lett. **102**, 076405 (2009).

23. O. Stockert, M. M. Koza, J. Ferstl et al., Physica B **378–380**, 157 (2006).

24. A. Hiess, O. Stockert, M. M. Koza et al., Physica B **378–380**, 748 (2006).

25. A. Steppke, R. Küchler, S. Lausberg et al., Science **339**, 933 (2013).

26. L. Isaev, K. Aoyama, I. Paul, and I. Vekhter, Phys. Rev. Lett. **111**, 157202 (2013).

27. V. A. Ivanshin, A. A. Sukhanov, D. A. Sokolov et al., J. Alloys Comp. **480**, 126 (2009).

28. S. V. Demishev, A. V. Semeno, A. V. Bogach et al., Diffusion and Defect Data B **152–153**, 353 (2009).

29. S. V. Demishev, A. V. Semeno, A. V. Bogach et al., Phys. Rev. B **80**, 245106 (2009).

30. H. Jang, G. Friemel, J. Ollivier et al., arXiv:cond-mat/1308.4491v1.

31. V. V. Glushkov, A. V. Semeno, N. E. Sluchanko et al., Physica B **403**, 932 (2008).